1521-009X/44/11/1819–1827$25.00
Drug Metabolism and Disposition

http://dx.doi.org/10.1124/dmd.116.071761
Drug Metab Dispos 44:1819–1827, November 2016

The Impact of the Hepatocyte-to-Plasma pH Gradient on the Prediction of Hepatic Clearance and Drug-Drug Interactions for CYP2D6 Substrates[S]

Luc R. A. Rougée, Michael A. Mohutsky, David W. Bedwell, Kenneth J. Ruterbories, and Stephen D. Hall

Lilly Research Laboratories, Eli Lilly and Company, Indianapolis, Indiana

Received May 26, 2016; accepted September 1, 2016

ABSTRACT

The proton gradient from the intracellular space to plasma creates an unbound drug gradient for weak acids and bases that could modulate apparent drug clearance and drug-drug interactions. Cytochrome P450 intrinsic clearance and inhibitor potency are routinely determined in vitro at the plasma pH of 7.4 rather than the intrahepatocyte pH of 7.0. We determined the impact of pH on in vitro enzyme kinetic parameters and inhibition potency for substrates (bufuralol, dextromethorphan), reversible inhibitors (quinidine, amiodarone, desethylamiodarone, clozapine), and mechanism-based inhibitors (paroxetine, desethylamiodarone) of the major drug metabolizing-enzyme CYP2D6. The lower intracellular pH 7.0 compared with pH 7.4 resulted in a 60 and 50% decrease in intrinsic clearance for the substrates bufuralol and dextromethorphan, respectively. Reversible inhibition constants for three of the four inhibitors tested were unaffected by pH, whereas for the inhibitor quinidine, a 2-fold increase in the inhibition constant was observed at pH 7.0. For time-dependent inhibitors desethylamiodarone and paroxetine, changes in time-dependent inhibition parameters were different for each inhibitor. These results were incorporated into physiologically based pharmacokinetic models indicating that the changes in in vitro parameters determined at pH 7.0 offset the effect of increased unbound intracellular concentrations on apparent clearance and extent of drug-drug interactions. However, this offset between concentration and enzyme activity cannot be generalized for all substrates, inhibitors, and enzymes, as the effect of a lower pH in vitro varied significantly; therefore, it would be prudent to determine in vitro enzyme parameters at the hepatocyte-appropriate pH 7.0.

Introduction

Physiologically based pharmacokinetic (PBPK) models, of various types, are widely used to predict absorption, in vivo drug clearance, volume of distribution, and the "shape" of plasma and tissue concentration versus time curves using in vitro and/or preclinical in vivo data (Jones and Rowland-Yeo, 2013). In these models, the dependence of factors such as intestinal fluid solubility, apparent intestinal permeability, and tissue membrane partitioning on pH has been taken into account (Rodgers et al., 2005; Chen et al., 2012). The intracellular pH is more acidic than that of plasma and interstitial fluid (Frieden, 1984; Hall and Guyton, 2015), and consequently, the unbound intracellular concentration, consisting of ionized and un-ionized species, will differ from that in plasma for drugs that exist in ionized and un-ionized forms at physiologic pH values (Shore et al., 1957). The ratio of the intracellular unbound concentration to the unbound plasma concentration, Kp_{uu}, can be readily calculated using the Henderson-Hasselbalch relationship under the assumptions that the permeability of the cell membrane to ionized drug is negligible and the distribution of un-ionized drug is only passive (Berezhkovskiy, 2011; Mateus et al., 2013). However, the implications of the pK_a-dependent Kp_{uu} for prediction of in vivo clearance from in vitro data are poorly understood.

The ionization factor (F_I) was developed to modify the in vitro–derived drug intrinsic clearance to account for the pK_a-dependent Kp_{uu} in the prediction of in vivo clearance (Berezhkovskiy, 2011). The use of F_I assumes that the only effect of the lower intracellular pH, relative to plasma, is to change the rate of elimination by modulating the product of unbound intracellular concentration and intrinsic clearance (Berezhkovskiy, 2011; Berezhkovskiy et al., 2012). However, this approach assumes that the in vitro intrinsic clearance of the eliminating pathway is estimated at the appropriate intracellular pH, or that intrinsic clearance is not affected by a pH over the range of 7.0–7.4. In addition, the F_I approach assumes that the rate of elimination is a function of the sum of the ionized and un-ionized forms of the unbound drug. Similarly, when the pK_a-dependent Kp_{uu} is used to modify the inhibition potency of a drug, it is assumed that the inhibitory constant is appropriately estimated, and that the sum of the ionized and un-ionized forms of the unbound drug is equally inhibitory.

Determination of the Michaelis-Menten constant (K_m), maximum rate of reaction (V_{max}), intrinsic clearance (CL_{int}), and inhibition constants [inhibitory constant for reversible inhibitors (K_i), inhibitory constant for time-dependent inhibition (K_I), and maximum rate of enzyme inactivation (k_{inact})] for cytochrome P450 (P450)–catalyzed reactions is routinely performed at pH 7.4 despite in vitro and in vivo observations that hepatocyte intracellular pH, including the cytosol and endoplasmic reticulum, is 7.0 (Park et al., 1979; Pollock, 1984; Bonventre and

dx.doi.org/10.1124/dmd.116.071761.
[S]This article has supplemental material available at dmd.aspetjournals.org.

ABBREVIATIONS: AUC, area under the plasma concentration-time curve; DDI, drug-drug interaction; HLM, human liver microsomes; LC-MS/MS, liquid chromatography–tandem mass spectrometry; P450, cytochrome P450; PBPK, physiologically based pharmacokinetic; PK, pharmacokinetic; QD, every day; TDI, time-dependent inhibition.

Cheung, 1985; Andersson et al., 1987; Fitz et al., 1992; Durand et al., 1993; Strazzabosco et al., 1995; Gerweck and Seetharaman, 1996; Kim et al., 1998; Vidal et al., 1998). Ionizable groups within P450 enzymes have the potential to modulate catalytic and inhibitory parameters as pH varies, and the relative affinity of the active site for ionized and un-ionized drug is unclear (Denisov et al., 2005). Berezhkovskiy et al. (2012) investigated the difference in fraction unbound and intrinsic clearance, through parent degradation, in rat liver microsomes at pH 7.0 and pH 7.4 for a set of seven proprietary compounds. Although differences were detected between the pH values, it was concluded that the results were within assay variability, and that the prediction of hepatic clearance using F_I could be used with intrinsic clearance values determined at pH 7.4. However, this interpretation was based on a small chemical space and unknown elimination pathways, and therefore, extending this conclusion to all in vitro metabolism studies is not presently justified.

The current study was undertaken to establish the impact of pH on these in vitro determinations for one of the major drug-metabolizing enzymes, CYP2D6. Enzyme kinetic parameters used for clearance (K_m, V_{max}, CL_{int}) were determined by metabolite formation in human liver microsomes (HLM) using two prototypical probe substrates, bufuralol and dextromethorphan. The inhibitory potential for reversible and time-dependent inhibitors (K_i, K_I, and k_{inact}) toward these substrates was also investigated. The in vitro findings were incorporated into PBPK models to predict exposure and drug-drug interactions (DDIs) in an effort to understand the significance of pH dependence of enzymes in the in vitro system in combination with the F_I correction.

Materials and Methods

Materials. Chemical reagents were obtained commercially: dextromethorphan, NADPH, quinidine, amiodarone, clozapine, paroxetine, and metoclopramide (Sigma-Aldrich, St. Louis, MO); bufuralol, 1′-hydroxybufuralol, and desethylamiodarone (Toronto Research Chemicals Inc., Toronto, Canada); dextrorphan (Cerilliant, Round Rock, TX); and sodium phosphate monobasic, sodium phosphate dibasic, phosphoric acid, and sodium hydroxide (Fisher Scientific, Pittsburgh, PA). A single lot of HLM pooled from 150 individuals (UltraPoolTM, lot #38290, equal proportion male and female; Corning, Tewksbury, MA) was used for all experiments.

In Vitro Incubations. Reactions were conducted in a shaking water bath at 37°C. Incubations were carried out in 100 mM sodium phosphate ($NaPO_4$) buffers adjusted to the pH of interest (6.0, 6.5, 7.0, 7.2, 7.4, 8.0, 8.5, 9.0) with phosphoric acid or sodium hydroxide as necessary. Linear conditions for metabolite formation with respect to time and protein at pH 6.0, pH 7.4, and pH 9.0 were determined for bufuralol and dextromethorphan, and are reflected in the final conditions described.

Substrates, buffer, and microsomes were premixed, and incubations were initiated by addition of the NADPH cofactor. In the case of reversible inhibition studies, inhibitor and cofactor were added at the initiation of the reaction simultaneously. Time-dependent inhibition studies were performed using the dilution method (Mohutsky and Hall, 2014). All incubations were carried out in 96-well plates in triplicate. Product formation (1′-hydroxybufuralol dextrorphan, 3-hydroxyquinidine) assays were performed on three separate occasions. Methanol (MeOH) was used as a solvent for all experiments at a final percent solvent percentage of less than 2% (v/v).

1′-Hydroxybufuralol Formation. Formation of 1′-hydroxybufuralol was determined using bufuralol (0.78–100 μM) and HLM (0.125 mg/ml) in 100 mM $NaPO_4$ buffer over a range of pH values between 6.0 and 9.0 (Crespi et al., 1998). The mixture was preincubated for 3 minutes at 37°C prior to reaction initiation through the addition of NADPH (1 mM, prepared in corresponding pH buffer), for a total volume of 150 μl. The reaction was allowed to proceed for 20 minutes at 37°C, at which time a 50 μl aliquot was added to 100 μl of 90:10 (v/v) MeOH:H_2O containing internal standard to stop the reaction. Plates were sealed with Easy Pierce 20 μm foil (Thermo Fisher Scientific, Waltham, MA), vortexed for 20 seconds, centrifuged (3500*g* for 10 minutes), and analyzed by liquid chromatography–tandem mass spectrometry (LC-MS/MS) (Supplemental Materials, Table S1). Reactions were performed in triplicate wells on three separate occasions. Metabolite formation was determined using a standard curve of 1′-hydroxybufuralol generated under identical conditions (0.5–1000 nM).

Dextrorphan Formation. Formation of dextrorphan from dextromethorphan (Schmider et al., 1997) was determined using the same procedure as described earlier for 1′-hydroxybufuralol with the following changes: dextromethorphan (0.39–50 μM) and HLM (0.1 mg/ml) in 100 mM $NaPO_4$ buffer at pH 6.0–9.0 were used; after preincubation and initiation, reactions proceed for 10 minutes at 37°C before being stopped. Metabolite formation was determined using a standard curve of dextrorphan generated under identical conditions (0.5–500 nM).

3-Hydroxyquinidine Formation. Formation of 3-hydroxyquinidine from quinidine was measured, as it is the major metabolite of quinidine metabolism and is only formed via CYP3A4 in vitro (Nielsen et al., 1999). Formation was determined at pH 7.0 and pH 7.4 as described for 1′-hydroxybufuralol formation, with the following changes: quinidine (1.95–250 μM) and HLM (0.1 mg/ml) in 100 mM $NaPO_4$ buffer at pH 7.0 or 7.4 were incubated at 37°C for 20 minutes after reaction initiation. Reaction aliquots (30 μl) were added to 150 μl of 90:10 (v/v) MeOH:H_2O containing internal standard to stop the reaction. Metabolite formation was determined using a standard curve of 3-hydroxyquinidine generated under identical conditions (0.98–2000 nM).

Reversible Inhibition (K_i Determination). The equilibrium inhibition constant (K_i) was determined at pH 7.0 and pH 7.4 for four reversible inhibitors (quinidine, amiodarone, desethylamiodarone, clozapine). Bufuralol or dextromethorphan (3.125, 6.25, 12.5, and 50 μM) and HLM (0.125 and 0.1 mg/ml, respectively) in 100 mM $NaPO_4$ buffer at pH 7.0 or 7.4 were prepared and kept on ice. After preincubation (3 minutes at 37°C), inhibitor [quinidine (0–0.2 μM), amiodarone (0–200 μM), desethylamiodarone (0–100 μM), or clozapine (0–100 μM)] was added with NADPH (1 mM prepared in corresponding buffer) (Fowler and Zhang, 2008). Reactions proceeded for 20 minutes for bufuralol and 10 minutes for dextromethorphan. Reaction (50 μl) was stopped through the addition of 100 μl of 90:10 (v/v) MeOH:H_2O containing internal standard. Plates were sealed with Easy Pierce 20 μm foil (Thermo Fisher Scientific), vortexed for 20 seconds, centrifuged (3500*g* for 10 minutes), and analyzed by LC-MS/MS (Supplemental Materials, Table S1).

Time-Dependent Inhibition (K_I and k_{inact} Determination). The maximum rate of enzyme inhibition (k_{inact}) and inhibitor concentration at which half the maximal rate of inactivation occurs (K_I) were determined for CYP2D6 using the dilution method (Mohutsky and Hall, 2014). In brief, perpetrator compounds [desethylamiodarone (0–50 μM), paroxetine (0–5 μM), metoclopramide (0–200 μM)] were incubated at 37°C with pooled HLM (0.5 mg/ml) and NADPH (1 mM) in 100 mM $NaPO_4$ buffer at pH 7.0 or 7.4 for 0, 2.5, 5, 15, and 30 minutes. After preincubation, a 10-fold dilution into a secondary incubation containing 50 μM bufuralol or 50 μM dextromethorphan with NADPH (1 mM) in corresponding buffer at pH 7.0 or 7.4 was performed. The secondary incubation was allowed to proceed for 10 minutes at 37°C, then an aliquot (50 μl) was added to 100 μl of 90:10 (v/v) MeOH:H_2O containing internal standard to stop the reaction. Plates were sealed with Easy Pierce 20 μm foil (Thermo Fisher Scientific), vortexed for 20 seconds, centrifuged (3500*g* for 10 minutes), and analyzed by LC-MS/MS (Supplemental Materials, Table S1).

Fraction Unbound in Microsomes. The fraction unbound in microsomes (fu_{mic}) was determined using a 96-well Micro-Equilibrium Dialysis Device HTD 96 (HTDialysis LLC, Gales Ferry, CT) per the manufacturer's instructions at HLM protein concentrations of 0.1 mg/ml for dextromethorphan, 0.5 mg/ml for metoclopramide and paroxetine, and 0.125 mg/ml for all other compounds. HLM were prepared in 100 mM $NaPO_4$ buffer at pH 7.0 or 7.4 containing 1 μM test drug and 100 μl added to one side of the dialysis membrane. The corresponding buffer (pH 7.0 or pH 7.4; 100 μl) was placed on the opposite side of the dialysis membrane. Samples (n = 6 replicates per day, repeated on three separate runs) were incubated in a shaking incubator (400 rpm) at 37°C for 4 hours using regenerated cellulose dialysis membranes (molecular weight cutoff 6–8 K). After incubation, aliquots from microsomes and buffer sides were taken and quenched into 90:10 (v/v) MeOH:H_2O containing internal standards. Plates were sealed with Easy Pierce 20 μm foil (Thermo Fisher Scientific), vortexed for 20 seconds, centrifuged (3500*g* for 10 minutes), and analyzed by LC-MS/MS (Supplemental Materials, Table S1).

PBPK Simulations. The population-based PBPK simulator Simcyp (V14; Certara, Princeton, NJ) was used to simulate exposure and DDI. Three separate

simulation scenarios were performed based on 1) baseline Simcyp compound file ($Sim_{pH\ 7.4}$), 2) baseline Simcyp compound file with the incorporation of F_I correction ($Sim_{pH\ 7.4,\ FI}$), and 3) baseline Simcyp compound file corrected as described later using in vitro results from pH 7.0 and 7.4 in the current study to correct baseline compound file ($Sim_{pH\ 7.0,\ FI}$).

The ionization factor was calculated as described by Berezhkovskiy (2011) as the ratio of ionized drug fractions in plasma to intracellular hepatocyte space by eq. 1:

$$F_I = \frac{1 - f_p^i}{1 - f_h^i} \quad (1)$$

where f_p^i and f_h^i are the fraction of charged (ionized) drug in the plasma (p) and intracellular hepatocyte space (h), respectively. The fraction of ionized drug was determined using the Henderson-Hasselbalch equation for monoprotic bases (eq. 2)

$$f_{base}^i = \frac{1}{1 + 10^{pH - pK_a}} \quad (2)$$

and the diprotic bases (eq. 3) quinidine and metoclopramide

$$f_{\substack{diprotic \\ base}}^i = \frac{1}{1 + \left[10^{pK_{a1} - pH} + 10^{pK_{a2} - pH} + 10^{pK_{a1} + pK_{a2} - 2pH}\right]^{-1}} \quad (3).$$

The pH values were 7.4 for plasma and 7.0 for the intracellular hepatocyte space.

The pH-specific in vitro CL_{int} ($CL_{int\ in\ vitro\ pH}$) was calculated as shown in eq. 4 using K_m, fu_{mic}, and V_{max} values determined at pH 7.0 or 7.4:

$$CL_{int\ in\ vitro\ pH} = \frac{V_{max\ in\ vitro\ pH}}{K_{m\ in\ vitro\ pH} \times fu_{mic\ pH}} \quad (4)$$

To account for the kinetic parameter changes (K_m, V_{max}) and fu_{mic} at the specific pH, assuming that all bottom-up data in the Simcyp files were generated at pH 7.4, eq. 5 describes the calculations used for the intrinsic clearances of the victim drugs, dextromethorphan and bufuralol. For dextromethorphan, the CYP2D6 HLM CL_{int} ($CL_{int,\ Simcyp}$) value provided in the elimination characteristics of the baseline Simcyp compound file and our own in vitro data were used to calculate an adjusted CL_{int} for the pH 7.0 simulations:

$$\text{Simulation } CL_{int\ pH\ 7.0} = \left(\frac{CL_{int\ in\ vitro\ pH\ 7.0}}{CL_{int\ in\ vitro\ pH\ 7.4}}\right) \times \left(CL_{int\ Simcyp}\right) \quad (5)$$

In the case of bufuralol, the baseline Simcyp bufuralol file was used as a starting point. Enzyme-specific pharmacokinetic (PK) parameters (V_{max} and K_m), determined in a recombinant system, for the conversion of bufuralol to either the metabolite 1′hydroxybufuralol or 6′-hydroxybufuralol are provided in the elimination characteristics of the compound file. These PK parameters were used to calculate a CL_{int} (V_{max}/K_m) for each enzyme isoform and metabolite pathway combination (e.g., a separate CL_{int} for CYP2D6 conversion of bufuralol to 1′hydroxybufuralol and 6′-hydroxybufuralol was determined). Since the contribution of the 6′-hydroxybufuralol metabolic pathway toward the total clearance is minor (~3%), the calculated CL_{int} values for the 1′hydroxybufuralol and 6′-hydroxybufuralol for each isoform were combined to provide a total CL_{int} ($CL_{int\ total}$) for each of the individual recombinant enzyme isoforms. Each enzyme isoform $CL_{int\ total}$ was converted to an HLM $CL_{int\ total}$ by using the relative abundance of the enzyme isoform per milligram of protein from the healthy volunteers population. This provided a fraction metabolized (f_m) for CYP2D6 of 0.617, which is much lower than the literature-calculated f_m of 0.83 based on extensive metabolizer/poor metabolizer ratios (Dayer et al., 1985, 1986). To compensate, CYP2D6 $CL_{int\ total}$ was increased to achieve an f_m of 0.83, whereas CYP2C19 $CL_{int\ total}$ was decreased to maintain the same total clearance of all isoforms combined. This new value for CYP2D6 $CL_{int\ total}$ was used for the simulations, and eq. 5 was used to calculate changes with regard to pH 7.0 (Supplemental Material, Table S2 and Fig. S1).

Simcyp baseline files for clozapine and paroxetine were used, and only the inhibition parameters (K_i, K_I, k_{inact}, and fu_{mic}) determined in vitro at the different pH values were altered in these files. In the case of quinidine, the baseline Simcyp compound file was used and the changes in inhibition parameters made. Additionally, the elimination through the major pathway (formation of 3-hydroxyquinidine by CYP3A4) was altered, based on our in vitro findings at pH 7.0 and pH 7.4, in the same manner as described earlier for dextromethorphan.

Compound files for amiodarone and desethylamiodarone were built as described by Chen et al. (2015) with the following exceptions: amiodarone and desethylamiodarone were categorized as monoprotic bases with pK_a values of 8.47 and 9.4, respectively, and the fraction available from dosage form (f_a) was increased from 0.6 to 0.8, as it provided a better fit to the clinical data from Andreasen et al. (1981) and Haffajee et al. (1983).

The ionization correction proposed by Berezhkovskiy (2011) was calculated based on the physicochemical properties of the compounds (acid/base; pK_a) and the pH of the intracellular (7.0) and extracellular (7.4) compartments (Table 1). This F_I value was then incorporated into the elimination section of the compound file as an *active uptake into hepatocytes*. This value alters the intracellular concentration of the compound by changing the Kp_{uu} to compensate for the difference in pH between the extracellular and intracellular compartments.

Simulation dosing schedules were chosen to mimic clinical dosage and/or clinical DDI studies, if available; however, for bufuralol, a literature search did not identify any DDI studies, and therefore, the dextromethorphan DDI study design information was used for bufuralol. All simulations were performed using the Simcyp healthy volunteer population using a 10-by-10 subject trial setup (total population size 100; equal portion male/female, age range 20–50 year) in the fasted state.

Inhibition by quinidine followed the study design from Abdul Manap et al. (1999), whereby a single dose of quinidine (50 mg) was given 1 hour prior to administration of bufuralol (60 mg) or dextromethorphan (30 mg) and followed for 96 hours. For clozapine, a single dose (12.5, 400, or 900 mg to represent possible dosing range) was given simultaneously with bufuralol (60 mg) or dextromethorphan (30 mg) and simulated for a 24-hour period (Perry et al., 1991). Interaction with amiodarone followed the study by Funck-Brentano et al. (1991), where a 1000 mg loading dose was given every day (QD) for 10 days followed by a 400 mg maintenance dose QD for 10 days. On day 20, a single dose of bufuralol (60 mg) or dextromethorphan (40 mg) was given, and the simulation proceeded for 24 hours after victim drug dosing. Paroxetine interaction followed the study format of Liston et al. (2002), where paroxetine (20 mg) was given QD for 10 days

TABLE 1

Physicochemical properties of the CYP2D6 substrates and inhibitors

Compound	pK_a1/pK_a2	Ionization Factor	Designation
Bufuralol	8.97[a]	2.472	Substrate
Dextromethorphan	8.3[a]	2.343	Substrate
Quinidine	4.2/8.8[a]	2.456	Reversible inhibitor
Amiodarone	8.47[b]	2.393	Reversible inhibitor
Desethylamiodarone	9.4[b]	2.497	Reversible inhibitor; time-dependent inhibitor
Clozapine	7.75[a]	2.045	Reversible inhibitor
Paroxetine	9.66[a]	2.504	Reversible inhibitor; time-dependent inhibitor
Metoclopramide	0.6/9.3[c]	2.493	Reversible inhibitor; time-dependent inhibitor

[a]Source: Simcyp.
[b]Source: The Human Metabolome Database (http://www.hmdb.ca).
[c]Foye et al. (2013).

followed by dextromethorphan (30 mg) or bufuralol (60 mg) on day 10 and followed for 24 hours.

Statistical Analysis. The HLM enzyme kinetic parameters (V_{max}, K_m, and CL_{int}) for bufuralol, dextromethorphan, and quinidine, as well as fu_{mic} values for all drugs, represent the mean of triplicate runs. Mean values of the replicates for pH 7.0 and 7.4 were analyzed for statistical differences with an unpaired, two-tailed *t* test using GraphPad Prism version 6.05 (GraphPad Software, San Diego, CA) using $\alpha = 0.05$. The ratio of the values obtained at pH 7.0 to values obtained at pH 7.4 is represented in the text of the results section as $Ratio_{7.0:7.4}$.

Results

Impact of pH on CYP2D6 Enzyme Kinetics. Enzyme kinetic parameters K_m, V_{max}, and CL_{int} varied with incubation pH, but the changes did not correlate with an increased abundance of ionized or un-ionized bufuralol and dextromethorphan (Fig. 1). The greatest affinity (lowest K_m) was observed at pH 8.0 for both substrates (Fig. 1, C and D), whereas V_{max} peaked at pH 7.4 and pH 7.2 for bufuralol and dextromethorphan, respectively (Fig. 1, E and F). This resulted in CL_{int} being highest at pH 8.0 for bufuralol and pH 7.4 for dextromethorphan (Fig. 1, G and H). Comparing pH values 7.0 and 7.4, represented as the ratio of the values obtained at pH 7.0 to values obtained at pH 7.4 ($Ratio_{7.0:7.4}$), K_m was increased (lower affinity) at pH 7.0 compared with pH 7.4, with a $Ratio_{7.0:7.4}$ of 1.3 and 2 for bufuralol and dextromethorphan, respectively. Conversely, the V_{max} was decreased at pH 7.0 compared with pH 7.4 for bufuralol ($Ratio_{7.0:7.4} = 0.6$) but remained relatively unchanged for dextromethorphan ($Ratio_{7.0:7.4} = 1.1$). The calculated CL_{int} was lower at pH 7.0 compared with pH 7.4 for both substrates, with a $Ratio_{7.0:7.4}$ of 0.4 and 0.5 for bufuralol and dextromethorphan, respectively. This decrease in CL_{int} was statistically significant between the two pH values for both bufuralol ($P = 0.004$) and dextromethorphan ($P < 0.001$).

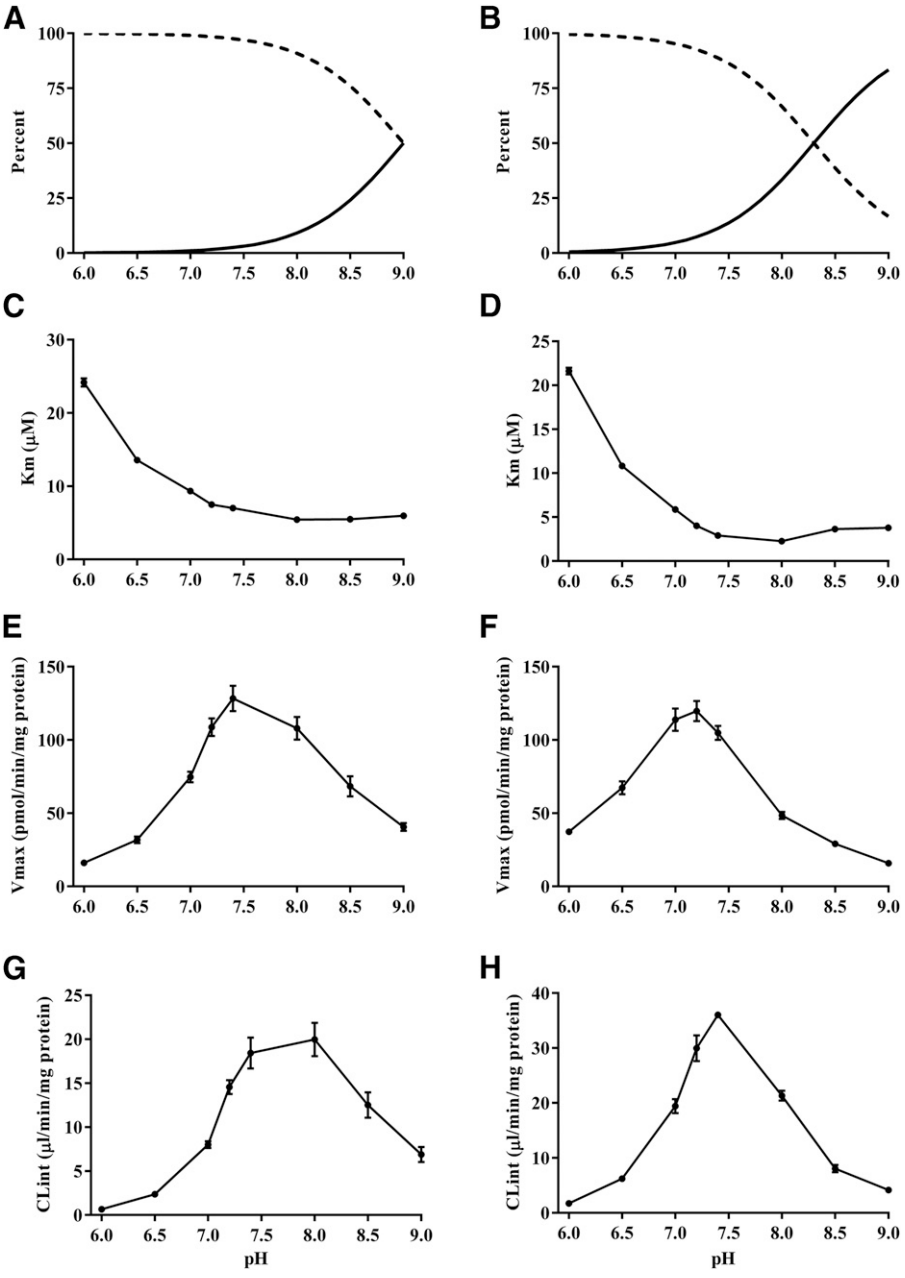

Fig. 1. Effect of pH on CYP2D6 enzyme kinetic parameters. (A) Calculated percentage of bufuralol (base, $pK_a = 9.0$) ionized and un-ionized species. (B) Calculated percentage of dextromethorphan (base, $pK_a = 8.3$) ionized and un-ionized species. (C) K_m of 1′-hydroxybufuralol formation from bufuralol. (D) K_m of dextrorphan formation from dextromethorphan. (E) V_{max} of 1′-hydroxybufuralol formation from bufuralol. (F) V_{max} of dextrorphan formation from dextromethorphan. (G) CL_{int} of 1′-hydroxybufuralol formation from bufuralol. (H) CL_{int} of dextrorphan formation from dextromethorphan. Dashed line represents the percentage ionized of the substrate; solid line represents the percentage un-ionized of the substrate. Symbols represent the mean of triplicate determinations, with vertical bars representing S.E.M.

TABLE 2

Reversible CYP2D6 inhibition kinetic parameters at pH 7.0 and pH 7.4.

Ratio between pH 7.0 and pH 7.4 results are given.

Substrate/Inhibitor	$fu_{mic\ pH\ 7}$	$K_{i,u\ pH\ 7}$	$fu_{mic\ pH\ 7.4}$	$K_{i,u\ pH\ 7.4}$	$K_{i,u}$
		μM		*μM*	*Ratio*
Bufuralol					
Quinidine	0.934	0.090	0.939	0.041	2.21
Amiodarone	0.0020	0.096	0.0016	0.112	0.86
Desethylamiodarone	0.0046	0.078	0.0043	0.087	0.89
Clozapine	0.843	28.6	0.830	28.4	1.01
Paroxetine	0.493[a]	0.46	0.410[a]	0.33	1.39
Dextromethorphan					
Quinidine	0.946[a]	0.051	0.951[a]	0.026	1.95
Amiodarone	0.0026[a]	0.083	0.0020[a]	0.134	0.62
Desethylamiodarone	0.0057[a]	0.043	0.0054[a]	0.034	1.27
Clozapine	0.870[a]	14.9	0.859[a]	15.6	0.96
Paroxetine	0.549[a]	0.32	0.465[a]	0.28	1.14

[a] fu_{mic} for inhibitor under in vitro assay conditions calculated from Austin et al. (2002).

Although fu_{mic} differed between pH values, no statistical significance was reached in the fraction unbound between pH 7.0 and pH 7.4 for bufuralol, dextromethorphan, clozapine, quinidine, desethylamiodarone, and metoclopramide. A statistically significantly higher fu_{mic} was determined for pH 7.0 compared with pH 7.4 for amiodarone ($Ratio_{7.0:7.4} = 1.3$; $P = 0.001$) and paroxetine ($Ratio_{7.0:7.4} = 1.3$; $P = 0.003$). When pH 7.0 and pH 7.4 results were corrected for fraction unbound in microsomes, the previously described ratios were unaffected, with the exception of the $Ratio_{7.0:7.4}$ for the K_m for bufuralol, which increased from 1.3 to 1.4.

Impact of pH on Quinidine Metabolism. The enzyme kinetic parameters for quinidine metabolism were significantly different ($P < 0.001$ for K_m and V_{max}, respectively) between pH 7.0 ($K_m = 398.8$ μM; $V_{max} = 671.8$ pmol/min/mg protein) and pH 7.4 ($K_m = 72.3$ μM; $V_{max} = 1094.0$ pmol/min/mg protein). This resulted in a statistically significant decrease ($P < 0.001$) in the CL_{int} at pH 7.0 (1.7 μl/min/mg protein) compared with CL_{int} at pH 7.4 (15.3 μl/min/mg protein) with a $Ratio_{7.0:7.4}$ of 0.1.

Impact of pH on CYP2D6 Inhibition. Reversible inhibition, described by unbound corrected K_i ($K_{i,u} = K_i \cdot fu_{mic}$), did not appear to be significantly affected by the change in pH for the victim compound bufuralol with perpetrators amiodarone, desethylamiodarone, and clozapine, or dextromethorphan with clozapine (Table 2). A slight increase in inhibitor potency at pH 7.0 was observed for the perpetrator/victim combination of amiodarone/dextromethorphan ($Ratio_{7.0:7.4} = 0.6$), whereas a slight decrease in inhibitor potency at pH 7.0 was determined for desethylamiodarone/dextromethorphan ($Ratio_{7.0:7.4} = 1.3$). However, the $K_{i,u}$ for quinidine was approximately 2-fold higher (weaker inhibition) at pH 7.0 compared with pH 7.4 for both bufuralol ($Ratio_{7.0:7.4} = 2.2$) and dextromethorphan ($Ratio_{7.0:7.4} = 2.0$).

Despite reports of metoclopramide as a time-dependent inhibitor (TDI) (Desta et al., 2002; Berry and Zhao, 2008), in our hands, no evidence of time-dependent inhibition of CYP2D6 was observed. The unbound K_I ($K_{I,u} = K_I \cdot fu_{mic}$) of paroxetine was higher (decreased potency) at pH 7.0 compared with pH 7.4 ($Ratio_{7.0:7.4}$ of 1.7 and 2.4 for bufuralol and dextromethorphan, respectively, as the victim drug), whereas k_{inact} was unaffected for bufuralol ($Ratio_{7.0:7.4} = 0.9$) and dextromethorphan ($Ratio_{7.0:7.4} = 1.0$) as the victim drug (Fig. 2; Table 3). This trend was reversed with the TDI perpetrator desethylamiodarone, where $K_{I,u}$ was unaffected ($Ratio_{7.0:7.4}$ of 1.1 and 0.9 for bufuralol and dextromethorphan, respectively), but k_{inact} was higher (greater rate of enzyme inactivation) at pH 7.0 for both bufuralol ($Ratio_{7.0:7.4} = 1.4$) and dextromethorphan ($Ratio_{7.0:7.4} = 1.7$) (Fig. 2; Table 3). No reversible inhibition at time zero for the secondary incubation was observed for desethylamiodarone or metoclopramide TDI experiments. However, some reversible inhibition was observed for the two highest concentrations of paroxetine (5 and 2.5 μM, with activity inhibited by 45 and 30%, respectively, compared with controls).This was expected due to final concentrations of paroxetine in the secondary incubation being close to K_i after dilution.

PBPK Simulations Using In Vitro Parameters. The simulations including the F_I correction alone for bufuralol and dextromethorphan predicted a 2-fold lower exposure of drug given by the area under the concentration-time profile curve (AUC). A 0.4- and 0.5-fold difference between $Sim_{pH\ 7.4,\ FI}$ and $Sim_{pH\ 7.4}$, respectively, was observed when the

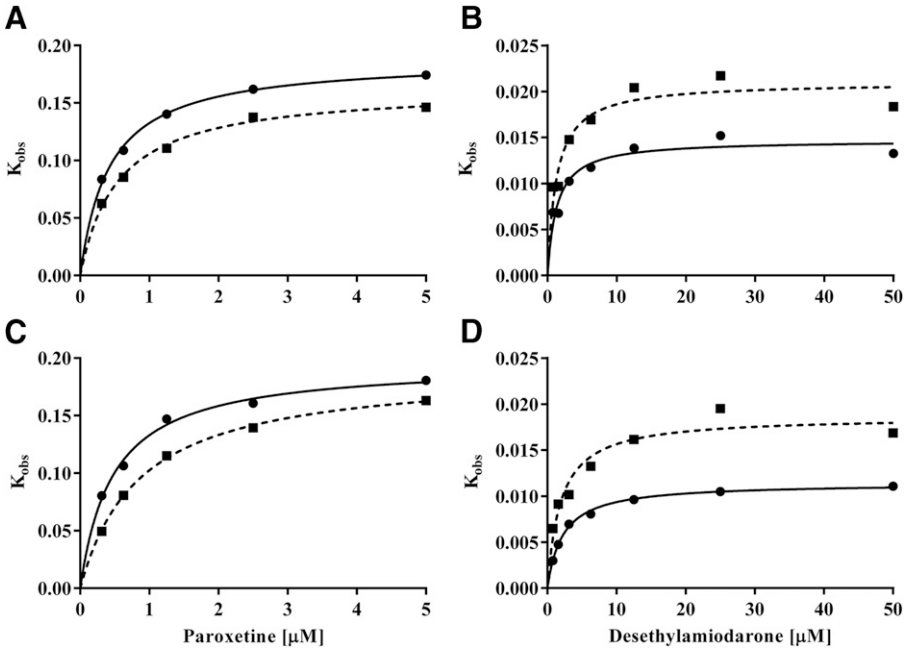

Fig. 2. Pseudo first-order inhibition rate constants for loss of CYP2D6 activity versus inhibitor concentration performed at pH 7.0 (dashed line with square symbols) and pH 7.4 (solid line with circle symbols). (A) Paroxetine inhibition of 1′-hydroxybufuralol formation from bufuralol. (B) Desethylamiodarone inhibition of 1′-hydroxybufuralol formation from bufuralol. (C) Paroxetine inhibition of dextrorphan formation from dextromethorphan. (D) Desethylamiodarone inhibition of dextrorphan formation from dextromethorphan. Symbols represent mean of triplicates.

TABLE 3

Time-dependent CYP2D6 inhibition kinetic parameters at pH 7.0 and pH 7.4

Results for the ratio between pH 7.0 and pH 7.4 are given.

Substrate/Inhibitor	$fu_{mic\ pH\ 7}$	$K_{I,u\ pH\ 7}$	$k_{inact\ pH\ 7}$	$fu_{mic\ pH\ 7.4}$	$K_{I,u\ pH\ 7.4}$	$k_{inact\ pH\ 7.4}$	$K_{I,u}$	K_{inact}
		nM	min^{-1}		*nM*	min^{-1}	*Ratio*	*Ratio*
Bufuralol								
Paroxetine	0.196	106.43	0.163	0.148	62.60	0.189	1.70	0.86
Desethylamiodarone	0.0011[a]	1.47	0.021	0.0011[a]	1.41	0.015	1.05	1.40
Dextromethorphan								
Paroxetine	0.196	167.38	0.190	0.148	70.30	0.196	2.38	0.97
Desethylamiodarone	0.0011[a]	2.19	0.019	0.0011[a]	2.38	0.011	0.92	1.73

[a]fu_{mic} for inhibitor under in vitro assay conditions prior to dilution (0.5 mg/mL) was calculated from Austin et al. (2002).

ionization correction was used, as a result of an increase in the rate of elimination due to a greater intracellular unbound concentration available in the hepatocyte (Fig. 3; Table 4). When pH 7.0 in vitro data were combined with the ionization correction, the calculated exposure for $Sim_{pH\ 7.0,\ FI}$ was within 20% of the $Sim_{pH\ 7.4}$ with an AUC fold difference of 0.8 for both bufuralol and dextromethorphan (Fig. 3; Table 4). The increase in intracellular unbound concentration due to the ionization correction was offset by the decrease in CL_{int} determined at pH 7.0.

The AUC ratios (AUC in the presence of inhibitor to absence of inhibitor) for the victim-perpetrator combinations are listed in Table 5. No significant change in AUC ratio was observed for clozapine, regardless of dosage (single dose of 12.5, 400, or 900 mg). Under the $Sim_{pH\ 7.4,\ FI}$ conditions, interaction studies showed a slight increase in AUC ratio for both bufuralol and dextromethorphan compared with $Sim_{pH\ 7.4}$ ($Ratio_{7.0:7.4}$ ranging from 1.2 to 1.5) for the amiodarone (including desethylamiodarone metabolite), quinidine, and paroxetine perpetrators. However, when $Sim_{pH\ 7.0,\ FI}$ conditions were used, the AUC ratio returned to the $Sim_{pH\ 7.4}$ observations for all perpetrators, with the exception of quinidine, which maintained the higher AUC ratio with dextromethorphan, and paroxetine, where a lower AUC ratio was determined for both bufuralol and dextromethorphan.

The lack of clinically observed DDI observations makes it difficult to assess the predictability of the models. The only clinical observations reported for dextromethorphan dosed alone as the victim are with quinidine as the perpetrator. Two studies which followed the same dosing design described in *Materials and Methods* (single 30 mg dose of dextromethorphan with single 50 mg dose of quinidine) observed a dextromethorphan AUC ratio of 16.2 (Abdul Manap et al., 1999) and 43 for extensive metabolizers (Capon et al., 1996). These interactions are significantly higher than the current model predictions, which range from 3.3 to 4.5 (Table 5). Additional clinical studies of various designs were modeled and resulted in an underprediction of the quinidine interaction (Supplemental Material, Table S3). The underprediction of quinidine suggests that other factors may influence the level of inhibition observed in vivo and highlights the importance of understanding all pharmacokinetic attributes of the victim and perpetrator compounds.

Discussion

Intracellular pH is consistently reported in the range of 6.8–7.2, depending on the cell and tissue type, with hepatocytes having an intracellular pH 7.0 in humans and animal species (Waddell and Bates, 1969; Park et al., 1979; Roos and Boron, 1981; Pollock, 1984; Bonventre and Cheung, 1985; Andersson et al., 1987; Fitz et al., 1992; Durand et al., 1993; Strazzabosco et al., 1995; Gerweck and Seetharaman, 1996; Vidal et al., 1998; Schmitt, 2008; Sanchez and Lopez-Zapata, 2015). Since plasma pH is 7.4, this results in a pH differential between plasma and the intracellular environment that theoretically would lead to a pK_a-dependent change in the ratio of intracellular unbound concentration to the unbound plasma concentration, or Kp_{uu}. In vitro evidence has been presented demonstrating the differential accumulation of diverse acid, base, and neutral compounds in support of the pH partitioning theory (Shore et al., 1957; Mateus et al., 2013). Since the liver is the major route of drug elimination, and given the phenomenon of Kp_{uu} changing based on the physicochemical properties of the drug and the pH of plasma and the hepatocyte, hepatic models for clearance can be modified to account for changes in intracellular concentration through an F_I correction (Berezhkovskiy, 2011).

Use of the F_I correction assumes that metabolism of a drug is driven by the sum of the ionized and un-ionized forms, and that the rate of reaction is not driven solely by a single species. This is not the case for the monoamine oxidase B enzyme that has been shown to predominantly metabolize the protonated (ionized) form of β-phenylethylamine (Jones et al., 2007). However, in our current study, a wide range of pH values

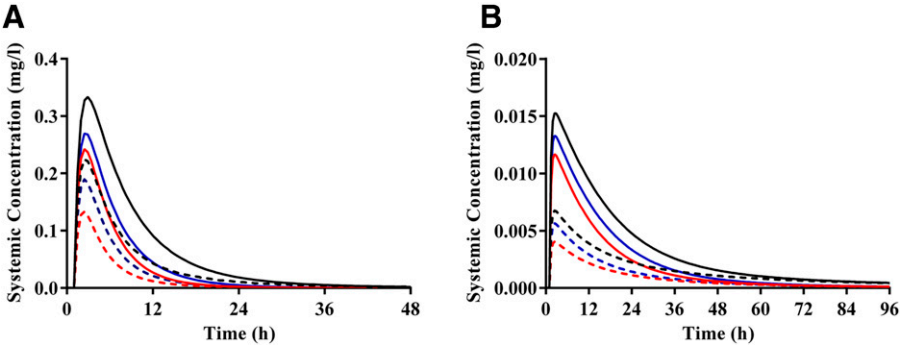

Fig. 3. Simulated plasma concentration time curves of bufuralol (A) and dextromethorphan (B) in the absence and presence of quinidine. Black lines represent baseline Simcyp compound file with pH 7.4 in vitro findings only; red lines represent baseline Simcyp compound file with pH 7.4 in vitro findings and the incorporation of F_I correction; blue lines represent baseline Simcyp compound file with pH 7.0 in vitro correction and the incorporation of F_I correction (see *Materials and Methods* for details). Dashed lines represent substrate concentration in the absence of quinidine; solid lines represent substrate concentration in the presence of quinidine.

TABLE 4

Simulated PK parameters for bufuralol and dextromethorphan

Dose of bufuralol (60 mg) or dextromethorphan (30 mg) simulation for 24 h. Geometric means reported with fold difference between simulation and traditional $Sim_{pH7.4}$ given in parentheses.

Simulation	Bufuralol				Dextromethorphan			
	$CL_{int,u}$	CL	C_{max}	AUC	$CL_{int,u}$	CL	C_{max}	AUC
	μl/min/mg protein	*l/h*	*μg/l*	*μg/l·h*	*μl/min/mg protein*	*l/h*	*μg/l*	*μg/l·h*
$Sim_{pH\ 7.4}$	20.0	49.02	209.02	1223.91	36.0	500.47	5.16	59.94
$Sim_{pH\ 7.4,\ FI}$	20.0 (1.0)	118.70 (2.4)	116.84 (0.6)	505.47 (0.4)	36.0 (1.0)	1085.39 (2.2)	2.61 (0.5)	27.64 (0.5)
$Sim_{pH\ 7,\ FI}$	8.3 (0.4)	64.72 (1.3)	180.45 (0.9)	927.01 (0.8)	19.4 (0.5)	630.14 (1.3)	4.28 (0.8)	47.61 (0.8)
Observed	—	66.96	164[a]	896[a]	—	845.1	3.49[b]	35.5[b]

CL, clearance calculated as dose/AUC; $CL_{int,u}$, in vitro intrinsic clearance corrected for fraction unbound in microsomes.
[a]Dayer et al. (1982).
[b]Chi et al. (2013).

(6.0–9.0) were used to investigate metabolism through CYP2D6. This range included considerable changes in the ratio of ionized and un-ionized forms of bufuralol and dextromethorphan. Evidence to suggest that a single species of either substrate was responsible for the metabolism was not observed. Therefore, the assumption was made that the total concentration of drug, the sum of the ionized and un-ionized species, drives the reaction, and the total concentration of intracellular drug can be used in the adjusted models for predictions.

An important caveat of studying the influence of pH is that both the charged state of the compound and the enzyme can be altered, which can result in differences in interactions. Enzyme activity changes with respect to pH have been demonstrated in the literature for P450 enzymes and vary between isoforms and substrates investigated. For example, 7-ethoxycoumarin *O*-deethylase activity peaks at pH 7.4 over the pH range of 7.0–8.5 in mice liver fractions (Greenlee and Poland, 1978), and whereas 6β-hydroxytestosertone formation in HLM is higher at pH 7.4 compared with pH 7.1, different oxidative pathways for testosterone meabolism peak at different pH values between 6.8 and 8.0 (Gemzik et al., 1990; Fisher et al., 2000). Our findings show that pH significantly impacts CYP2D6 as evidenced through changes in affinity and the rate of reaction, given by K_m and V_{max}, toward the substrates with respect to pH. These observations represent the net effect of the changes in the enzyme as well as changes in the substrate ionization ratio in the reaction. Therefore, regardless of which species (ionized or un-ionized) is metabolized or the state of the enzyme, if the in vitro measurements mimic the in vivo physiology, then these changes are accounted for and the results can be scaled without correcting for an in vitro bias, as they provide a more physiologically accurate measure of CL_{int}. Additionally, the buffering capacity, ionic strength, and buffer constituents can all influence the activity of enzymes differently (Gemzik et al., 1990; Maenpaa et al., 1998), and further investigations are needed to understand the influence of different buffer conditions in conjunction with changing pH.

This is in contrast to the work done by Berezhkovskiy et al. (2012), who investigated the difference in protein binding and intrinsic clearance at pH 7.0 and pH 7.4 for a set of seven proprietary compounds. Although changes were detected between the different pH values, Berezhkovskiy et al. concluded the results to be within assay variability, and the novel equations using F_I could be applied to in vitro values determined at pH 7.4. However, work presented here illustrates that significant changes in the measured in vitro parameters at pH 7.0 compared with pH 7.4 are reproducible and outside of assay variability. Changes appear to be on a case-by-case basis, and therefore, no general conclusion for all clearance pathways and drugs can be made. Further implementation of F_I with in vitro hepatocyte data improved in vivo predictions and led the author to question whether the intracellular pH of hepatocytes in vitro is maintained (Berezhkovskiy, 2011). The author hypothesized that a disproportionately large ratio of incubation buffer to hepatocyte cell surface area would destroy the pH gradient, resulting in an intracellular pH equivalent to the extracellular environment. Metabolic stability of six commercial drugs in hepatocytes incubated in buffer at pH 7.0 compared with pH 7.4 was not different. Berezhkovskiy et al. (2013) argued that depletion would theoretically be altered if hepatocytes were able to maintain an intracellular pH 7.0 with a higher external pH due to an increase or decrease in intracellular concentration, and lack of difference between the two incubation conditions indicated that intracellular pH of the hepatocytes reflected the extracellular pH. However, this conclusion is based on the assumption that the rate of metabolism is identical at each pH since the drug concentration would theoretically be the same in the intracellular and extracellular compartments if buffer pH matched intracellular pH. Our current results indicate that intrinsic clearance can be altered between the two pH values. Therefore, Berezhkovskiy's conclusion can only be supported by determining whether the intrinsic clearance of the compounds investigated is unaltered between the two pH values. Further work in our laboratory has indicated that one of the compounds investigated, diclofenac, has a metabolism sensitive to pH in

TABLE 5

Ratio of AUC in the presence and absence of inhibitor from simulations. Ratio between simulation and traditional $Sim_{pH7.4}$ given in parentheses.

Simulation	Bufuralol				Dextromethorphan			
	Clozapine[a]	Amiodarone	Quinidine	Paroxetine	Clozapine[a]	Amiodarone	Quinidine	Paroxetine
$Sim_{pH\ 7.4}$	1.04	4.43	2.04	4.19	1.14	6.42	3.34	6.93
$Sim_{pH\ 7.4,\ FI}$	1.06 (1.0)	5.50 (1.2)	2.40 (1.2)	5.00 (1.2)	1.21 (1.1)	9.61 (1.5)	4.47 (1.3)	10.21 (1.5)
$Sim_{pH\ 7,\ FI}$	1.04 (1.0)	3.33 (0.8)	1.93 (1.0)	2.69 (0.6)	1.17 (1.0)	7.32 (1.1)	3.92 (1.2)	4.81 (0.7)

[a]AUC ratios for 900 mg of clozapine dose given.

HLM (data publication in process), which would explain the difference observed for this compound (Berezhkovskiy et al., 2013).

Enzyme inhibition can also show a similar dependence on pH. Whereas differences in reversible inhibition between pH values were observed, these were mostly eliminated when correcting for fraction unbound at the specific pH with the exception of quinidine, which retained a 2-fold weaker inhibition at pH 7.0 compared with pH 7.4 for both bufuralol and dextromethorphan. Application of the F_I correction increased the intracellular concentration of quinidine, and this in isolation increased its inhibition potential. However, it was realized that the clearance of the inhibitor via CYP3A could also be affected at the different pH. Upon implementation of the change in metabolism and inhibition potential of quinidine, the change in metabolism of the victim drugs, and the ionization correction for both the victim and the perpetrator into the model, we found that the changes in intracellular concentration put forth by F_I were offset by the changes in PK and inhibition parameters at the intracellular pH 7.0. Furthermore, changes in TDI parameters varied inversely between the perpetrators investigated. Combined with the lack of change in the inhibition potential of some inhibitors, these findings reinforce that differences with respect to pH are not consistent and preclude generic conclusions toward inhibition in general.

Finally, PBPK models represent a convenient tool to incorporate the in vitro parameters necessary to make in vivo clearance and DDI predictions. Implementation of the F_I correction into these models resulted in a higher predicted intracellular concentration and hence an increase in the predicted rate of elimination, as well as a decreased plasma exposure and inhibition AUC ratio when using in vitro values determined at pH 7.4. Conversely, when using values determined at pH 7.0, the F_I increase in intracellular concentration was offset by the decrease in in vitro parameters measured at the lower pH and resulted in a plasma exposure and inhibition AUC ratio closer to that predicted without accounting for intracellular trapping or in vitro intrinsic clearance. This demonstrates that the assumption that in vitro intrinsic clearance is not affected by pH is inaccurate, at least for these enzyme and substrate combinations. Therefore, the implementation of a pK_a-dependent Kp_{uu} correction to account for a change in the rate of elimination of an ionizable drug must be applied to in vitro data generated at the correct hepatic intracellular pH 7.0. In the case of inhibitors, such as quinidine, in which in vitro assays tend to underpredict inhibition potency, the reasons remain unclear. We have demonstrated that the F_I correction cannot completely explain these in vitro to in vivo correlation disparities when combined with changes in the parameters measured at pH 7.0. This reveals the importance of using an integrated system that takes into account all of the different in vitro factors involved in making predictions (clearance of the compound, clearance of the inhibitor, fraction unbound, and inhibition potential) at the correct intracellular pH to make predictions based on physiologically accurate characteristics. It is recommend that in vitro parameters in drug discovery be determined at the physiologically appropriate intracellular pH 7.0, combined with an ionization correction, to provide a correct starting point from which to further explore other potential reasons for disparities between in vitro and in vivo outcomes.

Authorship Contributions

Participated in research design: Rougée, Mohutsky, Hall.

Conducted experiments: Rougée, Mohutsky, Bedwell, Ruterbories.

Contributed new reagents or analytic tools: Rougée, Mohutsky, Bedwell, Ruterbories.

Performed data analysis: Rougée, Mohutsky, Bedwell, Ruterbories, Hall.

Wrote or contributed to the writing of the manuscript: Rougée, Mohutsky, Bedwell, Ruterbories, Hall.

References

Abdul Manap R, Wright CE, Gregory A, Rostami-Hodjegan A, Meller ST, Kelm GR, Lennard MS, Tucker GT, and Morice AH (1999) The antitussive effect of dextromethorphan in relation to CYP2D6 activity. *Br J Clin Pharmacol* **48**:382–387.

Andersson BS, Aw TY, and Jones DP (1987) Mitochondrial transmembrane potential and pH gradient during anoxia. *Am J Physiol* **252**:C349–C355.

Andreasen F, Agerbaek H, Bjerregaard P, and Gøtzsche H (1981) Pharmacokinetics of amiodarone after intravenous and oral administration. *Eur J Clin Pharmacol* **19**:293–299.

Berezhkovskiy LM (2011) The corrected traditional equations for calculation of hepatic clearance that account for the difference in drug ionization in extracellular and intracellular tissue water and the corresponding corrected PBPK equation. *J Pharm Sci* **100**:1167–1183.

Berezhkovskiy LM, Liu N, and Halladay JS (2012) Consistency of the novel equations for determination of hepatic clearance and drug time course in liver that account for the difference in drug ionization in extracellular and intracellular tissue water. *J Pharm Sci* **101**:516–518.

Berezhkovskiy LM, Wong S, and Halladay JS (2013) On the maintenance of hepatocyte intracellular pH 7.0 in the in-vitro metabolic stability assay. *J Pharmacokinet Pharmacodyn* **40**: 683–689.

Berry LM and Zhao Z (2008) An examination of IC50 and IC50-shift experiments in assessing time-dependent inhibition of CYP3A4, CYP2D6 and CYP2C9 in human liver microsomes. *Drug Metab Lett* **2**:51–59.

Bonventre JV and Cheung JY (1985) Effects of metabolic acidosis on viability of cells exposed to anoxia. *Am J Physiol* **249**:C149–C159.

Capon DA, Bochner F, Kerry N, Mikus G, Danz C, and Somogyi AA (1996) The influence of CYP2D6 polymorphism and quinidine on the disposition and antitussive effect of dextromethorphan in humans. *Clin Pharmacol Ther* **60**:295–307.

Chen Y, Jin JY, Mukadam S, Malhi V, and Kenny JR (2012) Application of IVIVE and PBPK modeling in prospective prediction of clinical pharmacokinetics: strategy and approach during the drug discovery phase with four case studies. *Biopharm Drug Dispos* **33**:85–98.

Chen Y, Mao J, and Hop CE (2015) Physiologically based pharmacokinetic modeling to predict drug-drug interactions involving inhibitory metabolite: a case study of amiodarone. *Drug Metab Dispos* **43**:182–189.

Chi KN, Tolcher A, Lee P, Rosen PJ, Kollmannsberger CK, Papadopoulos KP, Patnaik A, Molina A, Jiao J, Pankras C, et al. (2013) Effect of abiraterone acetate plus prednisone on the pharmacokinetics of dextromethorphan and theophylline in patients with metastatic castration-resistant prostate cancer. *Cancer Chemother Pharmacol* **71**:237–244.

Crespi CL, Chang TK, and Waxman DJ (1998) CYP2D6-dependent bufuralol 1′-hydroxylation assayed by reversed-phase ion-pair high-performance liquid chromatography with fluorescence detection. *Methods Mol Biol* **107**:141–145.

Dayer P, Balant L, Kupfer A, Striberni R, and Leemann T (1985) Effect of oxidative polymorphism (debrisoquine/sparteine type) on hepatic first-pass metabolism of bufuralol. *Eur J Clin Pharmacol* **28**:317–320.

Dayer P, Kubli A, Kupfer A, Courvoisier F, Balant L, and Fabre J (1982) Defective hydroxylation of bufuralol associated with side-effects of the drug in poor metabolisers. *Br J Clin Pharmacol* **13**:750–752.

Dayer P, Leemann T, Küpfer A, Kronbach T, and Meyer UA (1986) Stereo- and regioselectivity of hepatic oxidation in man–effect of the debrisoquine/sparteine phenotype on bufuralol hydroxylation. *Eur J Clin Pharmacol* **31**:313–318.

Denisov IG, Makris TM, Sligar SG, and Schlichting I (2005) Structure and chemistry of cytochrome P450. *Chem Rev* **105**:2253–2277.

Desta Z, Wu GM, Morocho AM, and Flockhart DA (2002) The gastroprokinetic and antiemetic drug metoclopramide is a substrate and inhibitor of cytochrome P450 2D6. *Drug Metab Dispos* **30**:336–343.

Durand T, Gallis JL, Masson S, Cozzone PJ, and Canioni P (1993) pH regulation in perfused rat liver: respective role of Na(+)-H+ exchanger and Na(+)-HCO3- cotransport. *Am J Physiol* **265**: G43–G50.

Fisher MB, Campanale K, Ackermann BL, VandenBranden M, and Wrighton SA (2000) In vitro glucuronidation using human liver microsomes and the pore-forming peptide alamethicin. *Drug Metab Dispos* **28**:560–566.

Fitz JG, Lidofsky SD, Xie MH, and Scharschmidt BF (1992) Transmembrane electrical potential difference regulates Na+/HCO3- cotransport and intracellular pH in hepatocytes. *Proc Natl Acad Sci USA* **89**:4197–4201.

Fowler S and Zhang H (2008) In vitro evaluation of reversible and irreversible cytochrome P450 inhibition: current status on methodologies and their utility for predicting drug-drug interactions. *AAPS J* **10**:410–424.

Foye WO, Lemke TL, and Williams DA(2013) *Foye's Principles of Medicinal Chemistry,* Wolters Kluwer Health/Lippincott Williams & Wilkins, Philadelphia.

Frieden E (1984) *Biochemistry of the Essential Ultratrace Elements*, Plenum, New York.

Funck-Brentano C, Jacqz-Aigrain E, Leenhardt A, Roux A, Poirier JM, and Jaillon P (1991) Influence of amiodarone on genetically determined drug metabolism in humans. *Clin Pharmacol Ther* **50**:259–266.

Gemzik B, Halvorson MR, and Parkinson A (1990) Pronounced and differential effects of ionic strength and pH on testosterone oxidation by membrane-bound and purified forms of rat liver microsomal cytochrome P-450. *J Steroid Biochem* **35**:429–440.

Gerweck LE and Seetharaman K (1996) Cellular pH gradient in tumor versus normal tissue: potential exploitation for the treatment of cancer. *Cancer Res* **56**:1194–1198.

Greenlee WF and Poland A (1978) An improved assay of 7-ethoxycoumarin O-deethylase activity: induction of hepatic enzyme activity in C57BL/6J and DBA/2J mice by phenobarbital, 3-methylcholanthrene and 2,3,7,8-tetrachlorodibenzo-p-dioxin. *J Pharmacol Exp Ther* **205**:596–605.

Haffajee CI, Love JC, Canada AT, Lesko LJ, Asdourian G, and Alpert JS (1983) Clinical pharmacokinetics and efficacy of amiodarone for refractory tachyarrhythmias. *Circulation* **67**:1347–1355.

Hall JE and Guyton AC (2015) *Guyton and Hall Textbook of Medical Physiology*, 13th ed. Elsevier Health Sciences, Philadelphia, PA.

Jones H and Rowland-Yeo K (2013) Basic concepts in physiologically based pharmacokinetic modeling in drug discovery and development. *CPT Pharmacometrics Syst Pharmacol* **2**:e63.

Jones TZ, Balsa D, Unzeta M, and Ramsay RR (2007) Variations in activity and inhibition with pH: the protonated amine is the substrate for monoamine oxidase, but uncharged inhibitors bind better. *J Neural Transm (Vienna)* **114**:707–712.

Kim JH, Johannes L, Goud B, Antony C, Lingwood CA, Daneman R, and Grinstein S (1998) Noninvasive measurement of the pH of the endoplasmic reticulum at rest and during calcium release. *Proc Natl Acad Sci USA* **95**:2997–3002.

Liston HL, DeVane CL, Boulton DW, Risch SC, Markowitz JS, and Goldman J (2002) Differential time course of cytochrome P450 2D6 enzyme inhibition by fluoxetine, sertraline, and paroxetine in healthy volunteers. *J Clin Psychopharmacol* **22**:169–173.
Mäenpää J, Hall SD, Ring BJ, Strom SC, and Wrighton SA (1998) Human cytochrome P450 3A (CYP3A) mediated midazolam metabolism: the effect of assay conditions and regioselective stimulation by alpha-naphthoflavone, terfenadine and testosterone. *Pharmacogenetics* **8**:137–155.
Mateus A, Matsson P, and Artursson P (2013) Rapid measurement of intracellular unbound drug concentrations. *Mol Pharm* **10**:2467–2478.
Mohutsky M and Hall SD (2014) Irreversible enzyme inhibition kinetics and drug-drug interactions. *Methods Mol Biol* **1113**:57–91.
Nielsen TL, Rasmussen BB, Flinois JP, Beaune P, and Brosen K (1999) In vitro metabolism of quinidine: the (3S)-3-hydroxylation of quinidine is a specific marker reaction for cytochrome P-4503A4 activity in human liver microsomes. *J Pharmacol Exp Ther* **289**:31–37.
Park R, Leach WJ, and Arieff AI (1979) Determination of liver intracellular pH in vivo and its homeostasis in acute acidosis and alkalosis. *Am J Physiol* **236**:F240–F245.
Perry PJ, Miller DD, Arndt SV, and Cadoret RJ (1991) Clozapine and norclozapine plasma concentrations and clinical response of treatment-refractory schizophrenic patients. *Am J Psychiatry* **148**:231–235.
Pollock AS (1984) Intracellular pH of hepatocytes in primary monolayer culture. *Am J Physiol* **246**: F738–F744.
Rodgers T, Leahy D, and Rowland M (2005) Physiologically based pharmacokinetic modeling 1: predicting the tissue distribution of moderate-to-strong bases. *J Pharm Sci* **94**:1259–1276.
Roos A and Boron WF (1981) Intracellular pH. *Physiol Rev* **61**:296–434.
Sánchez JC and López-Zapata DF (2015) Effects of Adipokines and Insulin on Intracellular pH, Calcium Concentration, and Responses to Hypo-Osmolarity in Human Articular Chondrocytes from Healthy and Osteoarthritic Cartilage. *Cartilage* **6**:45–54.
Schmider J, Greenblatt DJ, Fogelman SM, von Moltke LL, and Shader RI (1997) Metabolism of dextromethorphan in vitro: involvement of cytochromes P450 2D6 and 3A3/4, with a possible role of 2E1. *Biopharm Drug Dispos* **18**:227–240.
Schmitt W (2008) General approach for the calculation of tissue to plasma partition coefficients. *Toxicol In Vitro* **22**:457–467.
Shore PA, Brodie BB, and Hogben CA (1957) The gastric secretion of drugs: a pH partition hypothesis. *J Pharmacol Exp Ther* **119**:361–369.
Strazzabosco M, Poci C, Spirlì C, Zsembery A, Granato A, Massimino ML, and Crepaldi G (1995) Intracellular pH regulation in Hep G2 cells: effects of epidermal growth factor, transforming growth factor-alpha, and insulinlike growth factor-II on Na+/H+ exchange activity. *Hepatology* **22**:588–597.
Vidal G, Durand T, Canioni P, and Gallis JL (1998) Cytosolic pH regulation in perfused rat liver: role of intracellular bicarbonate production. *Biochim Biophys Acta* **1425**:224–234.
Waddell WJ and Bates RG (1969) Intracellular pH. *Physiol Rev* **49**:285–329.

Address correspondence to: Luc R. A. Rougée, Eli Lilly and Company, Indianapolis, IN. E-mail: lrougee@lilly.com

Supplemental Data

The Impact of the Hepatocyte-to-Plasma pH Gradient on the Prediction of Hepatic Clearance and Drug-Drug Interactions for CYP2D6 Substrates

Luc R.A. Rougée, Michael A. Mohutsky, David W. Bedwell, Kenneth J. Ruterbories, Stephen D. Hall

Drug Metabolism and Disposition

Analytical instrumentation and general aspects of bioanalysis. Study samples were analyzed by LC-MS/MS using a Sciex API 6500 triple quadrupole mass spectrometer (Applied Biosystems/MDS; Foster City, CA) equipped with a TurboIonSpray interface, and operated in positive ion mode. The pumps were Shimadzu LC-10AD units with a SCL-10A controller (Kyoto, Japan), and a CTC PAL liquid handler (Zwingen, Switzerland) was used as the autosampler. Chromatography was performed at ambient temperature. All compounds were chromatographically separated using a Thermo Betasil Javelin C18 2x20 mm 5 micron HPLC column (Thermo Fisher Scientific; Waltham, MA), except for 3-hydroxyquinidine that utilized an Echelon Sprite C18 2.1x20mm, HPLC column (Analytical Sales and Services; Pompton Plains, NJ). Analytical details for mobile phase A, mobile phase B, Q1/Q3 transition, and collision energy are summarized in Table S1.

Table S1. Bioanalytical analysis details.

Compound	*Mobile Phase A (v:v)*	*Mobile Phase B*	*Q1*	*Q3*	*CE*
Bufuralol	Water:Formic acid (1000:1)	Methanol	262.1	188.1	23
1'-hydroxybufuralol	Water:Formic acid (1000:10)	Methanol	278.0	186.0	30
Dextromethorphan	Water:Formic acid (1000:1)	Methanol	272.2	215.0	35
Dextrorphan	Water:Formic acid (1000:1)	Methanol	258.1	201.1	30
Quinidine	Water:2M NH4CO3 (1000:25)	Acetonitrile	325.2	160.1	40
3-hydroxyquinidine	Trifluoroacetic acid:2M NH_4CO_3 (1000:4:0.5)	Acetonitrile	341.1	160.1	45
Amiodarone	Water:Formic acid (1000:1)	Methanol	646.1	588.0	65
Desethylamiodarone	Water:Formic acid (1000:1)	Methanol	618.1	547.1	26
Clozapine	Water:2M NH4CO3 (1000:25)	Acetonitrile	327.2	270.0	33
Paroxetine	Water:2M NH4CO3 (1000:25)	Acetonitrile	330.1	192.1	20

Table S2. Parameters used for PBPK modeling.

Physical/Chemical Properties	*Absorption & Distribution*	*Elimination*	*Interactions*
Bufuralol			
MW: 261.36	ka: 1.32	Enzyme kinetics: HLM	
Log $P_{o:w}$: 3.5	Model: Minimal PBPK	$CL_{int,\ CYP1A2}$: 6.3	
Type: MB	V_{ss}: 1.38	$CL_{int,\ CYP2B6}$: 0.0207	
pKa 1: 8.97		$CL_{int,\ CYP2C19}$: 3.9	
B:P: 0.68		$CL_{int,\ CYP2D6}$: 63.6[a]; 26.4[b]	
fu_p:0.19		$CL_{int,\ CYP3A4}$: 2.7	
Dextromethorphan			
MW: 271.4	ka:2.6	Enzyme kinetics: HLM	
Log $P_{o:w}$: 3.8	Model: Minimal PBPK	$CL_{int,\ CYP2B6}$: 4.7	
Type: MB	V_{ss}: 14.3	$CL_{int,\ CYP2C9}$: 0.9	
pKa 1: 8.3		$CL_{int,\ CYP2C18}$: 0.052	
B:P: 1.32		$CL_{int,\ CYP2C19}$: 0.117	
fu_p: 0.5		$CL_{int,\ CYP2D6}$: 253[a]; 136.3[b]	
		$CL_{int,\ CYP3A4}$: 4.3	
Quinidine			
MW: 324.4	ka: 3	Enzyme kinetics: HLM	
Log $P_{o:w}$: 2.88	Model: Minimal PBPK	$CL_{int,\ CYP2C9\ (N\text{-}oxide)}$: 0.4	CYP2D6 K_i: 0.0436 [a]; 0.0966 [b]
Type: DB	V_{ss}: Predicted using Method 1	$CL_{int,\ CYP2E1\ (N\text{-}oxide)}$: 0.52	CYP2D6 fu_{mic}: 0.857[a];0.846[b]
pKa 1: 4.2		$CL_{int,\ CYP3A4\ (N\text{-}oxide)}$: 2.6	CYP3A4 K_i: 40

pKa 2: 8.8 $CL_{int, CYP3A4 (3\text{-}OH)}$: 20.65[a]; 7.9[b] CYP3A4 fu_{mic}: 0.58

B:P: 0.88

fu_p: 0.203

---

[a]value determined at pH 7.4 value; [b]value determined at pH 7.0

B:P, blood-to-plasma ratio; CL_{int}, intrinsic clearance (µl/min/mg protein); DB, diprotic base; fu_{mic}, fraction unbound in microsomes; fu_p, fraction unbound in plasma; HLM, human liver microsomes; ka, first-order absorption rate constant (h^{-1}); K_i, inhibitory constant for reversible inhibition (µM); Log $P_{o:w}$, neutral species octanol: buffer partition coefficient; MB, monoprotic base; MW, molecular weight (g/mol); pKa, acid dissociation constant; V_{ss}, volume of distribution at steady state (l/kg). Method 1 is based after Poulin P, Theil FP (2002) Prediction of pharmacokinetics prior to in vivo studies 1. Mechanism-based prediction of volume of distribution. Journal of Pharmaceutical Sciences 91(1):129-156. For all compounds, a First-Order Absorption Model was used with Lag time (h) of 0, a fraction available from dosage (fa) of 1, and an unbound fraction of drug in enterocytes (fu_{gut}) of 1.

Table S3. Comparison of the AUC ratio predicted by the quinidine model under different dosing simulations to clinical interaction studies.

	Literature Reference					
Simulation	*Bosilkovska et al. (2014)*[a] *CYP2D6 EM*	*Bosilkovska et al. (2014)*[a] *CYP2D6 IM*	*Zawertailo et al. (2010)*[b]	*Pope et al. (2004)*[c]	*Pope et al. (2004)*[d]	*Pope et al. (2004)*[e]
$Sim_{pH\ 7.4}$	5.4	1.0	2.7	6.6	6.0	6.0
$Sim_{pH\ 7.4,\ FI}$	7.4	1.0	2.3	8.2	7.6	7.6
$Sim_{pH\ 7,\ FI}$	5.9	1.0	3.7	7.2	6.7	6.7
Observed	19.2	2.7	10	47.8	45.8	43.3

All simulations were performed using the Simcyp Healthy Volunteer Population using a 10 by 10 subject trial set up (total population size 100; equal portion male/female, age range 20-50 yr) in the fasted state.

[a]Dextromethorphan 10 mg single dose given alone or 2 hr after 200 mg of quinidine in extensive metabolizers only.

[b]Dextromethorphan 210 mg (3 mg/kg dose; calculated for 70 kg average adult) single dose given alone or after 100 mg of quinidine dosed QID for three days before in intermediate metabolizers only.

[c]Dextromethorphan 30 mg given BID alone or in combination with 75 mg of quinidine for 7 days.

[d]Dextromethorphan 45 mg given BID alone or in combination with 60 mg of quinidine for 7 days.

[e]Dextromethorphan 60 mg given BID alone or in combination with 60 mg of quinidine for 7 days.

Figure S1

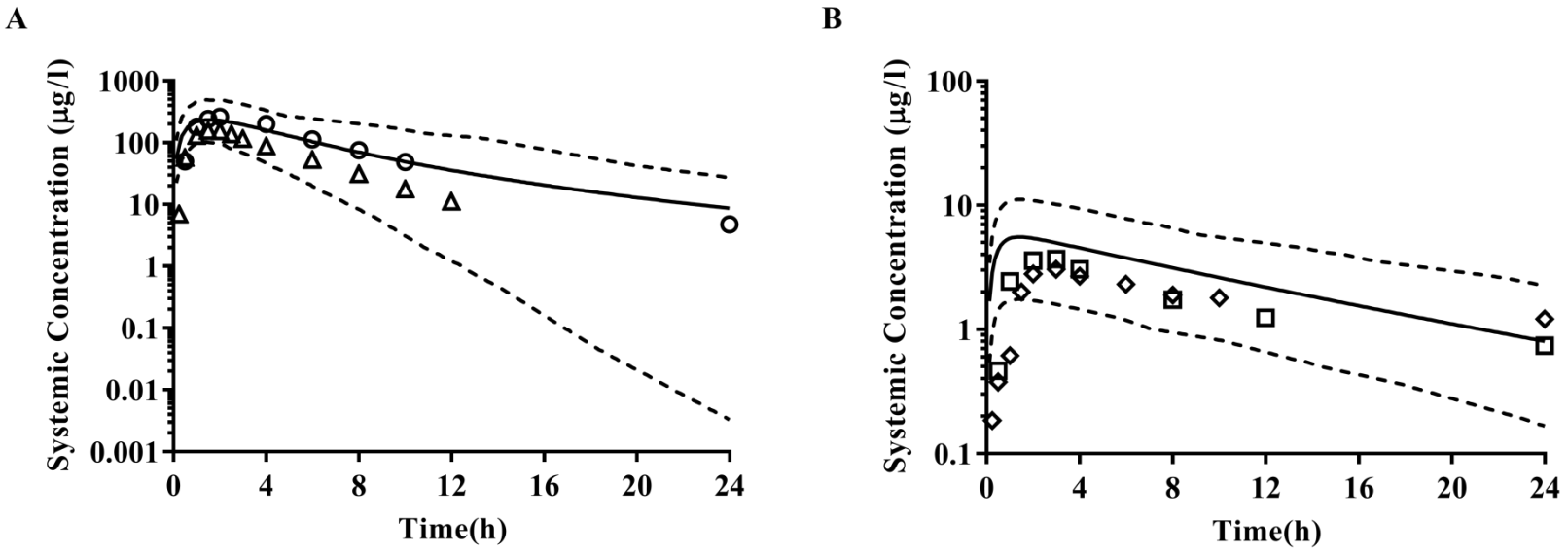

Figure S1. Predicted and observed plasma concentration-time profiles of A) bufuralol (60 mg) and B) dextromethorphan (30 mg). Solid and dashed lines represents the simulation average and 95 and 5% confidence interval respectively. Mean observed data from Pringle et al. (1986),(open circles) ; Dayer et al. (1985),(open triangles) ; Abdul Manap et al. (1999),(open squares) ; (Chi et al., 2013), (open diamonds).

References

Abdul Manap R, Wright CE, Gregory A, Rostami-Hodjegan A, Meller ST, Kelm GR, Lennard MS, Tucker GT, and Morice AH (1999) The antitussive effect of dextromethorphan in relation to CYP2D6 activity. *Br J Clin Pharmacol* **48:**382-387.

Bosilkovska M, Samer CF, Deglon J, Rebsamen M, Staub C, Dayer P, Walder B, Desmeules JA, and Daali Y (2014) Geneva cocktail for cytochrome p450 and P-glycoprotein activity assessment using dried blood spots. *Clin Pharmacol Ther* **96:**349-359.

Chi KN, Tolcher A, Lee P, Rosen PJ, Kollmannsberger CK, Papadopoulos KP, Patnaik A, Molina A, Jiao J, Pankras C, Kaiser B, Bernard A, Tran N, and Acharya M (2013) Effect of abiraterone acetate plus prednisone on the pharmacokinetics of dextromethorphan and theophylline in patients with metastatic castration-resistant prostate cancer. *Cancer Chemother Pharmacol* **71:**237-244.

Dayer P, Balant L, Kupfer A, Striberni R, and Leemann T (1985) Effect of oxidative polymorphism (debrisoquine/sparteine type) on hepatic first-pass metabolism of bufuralol. *Eur J Clin Pharmacol* **28:**317-320.

Pope LE, Khalil MH, Berg JE, Stiles M, Yakatan GJ, and Sellers EM (2004) Pharmacokinetics of dextromethorphan after single or multiple dosing in combination with quinidine in extensive and poor metabolizers. *J Clin Pharmacol* **44:**1132-1142.

Pringle TH, Francis RJ, East PB, and Shanks RG (1986) Pharmacodynamic and pharmacokinetic studies on bufuralol in man. *Br J Clin Pharmacol* **22:**527-534.

Zawertailo LA, Tyndale RF, Busto U, and Sellers EM (2010) Effect of metabolic blockade on the psychoactive effects of dextromethorphan. *Human psychopharmacology* **25:**71-79.